# Forced ignition of turbulent spray flames

E. Mastorakos*

*Hopkinson Lab, Department of Engineering, University of Cambridge, Trumpington Street, Cambridge CB2 1PZ, UK*

**Abstract**

This paper reviews the current state of knowledge on the initiation of a flame in a spray through the action of a spark or through local deposition of heat, and the subsequent flame development, in uniform and non-uniform dispersions of droplets and in the presence of turbulent flow. These processes are of importance in various applications such as gas turbine ignition (relight) and safety related to flammable liquid mists. The review focuses on the initial kernel development, the evolution of a spherical or edge flame, and the ignition of the spray flame when viewed at the whole combustor scale. The factors that determine success or failure of the ignition process at the various phases of the overall burner ignition are discussed through experiments and Direct Numerical Simulations, while modelling efforts are also assessed. The fuel volatility, droplet size, overall fuel-to-air ratio, and the degree of pre-evaporation are the important factors that distinguish spray ignition from gaseous flame ignition, and the extra fluctuations introduced by the random droplet locations, and how this may affect modelling and flame evolution, are highlighted. The flame propagation mechanism in laminar and turbulent sprays is one of the key aspects determining overall ignition success. Suggestions for future research are discussed.

*Keywords:* Forced ignition, Spark, Spray, Relight, Ignition probability, Modelling, Edge flame

*Corresponding author
*email address:* em257@eng.cam.ac.uk

## 1. Introduction

The initiation and subsequent complete establishment of combustion in a spray due to an externally-imposed means, such as an electrical or laser-induced spark, a plasma jet, or a heated surface, is here denoted as *forced ignition* and is reviewed from the perspective of the various temporal and spatial scales and the stochasticity of the underlying phenomena. This knowledge is not only of fundamental interest, but also of practical importance for a range of applications. One of these is the ignition in a gas turbine combustor. Especially for aviation gas turbines, the need to ensure ignition in the event of a flame extinction determines, to some extent, the operating envelope of the airplane and also the volume of the combustor. This, in turn, has implications for the weight, cost, and emissions of the engine. The need to be able to predict, at the design stage, the ignitability of a gas turbine combustor would be advantageous, but is limited at present by the complexity of the phenomena. As another example, we mention the danger of ignition in mists of a flammable liquid, where the assessment of an explosion hazard is not easily carried out in the absence of information on the ignition itself, but also the subsequent flame speed and the factors that affect both. This paper aims to review the present state of our knowledge on these topics, mostly from the point of view of the fundamentals behind spark ignition processes in spray systems and focusing on the effects of the spray and the turbulence on the initiation and evolution of the flame.

It is very important to distinguish the different phases involved in the ignition of a spray flame. These different phases can be summarized as follows [1, 2]:

1. Kernel generation
2. Flame growth
3. Burner-scale flame establishment

The boundaries between these phases are not always clear and this is amply manifested by the different interpretations given to the term *ignition* in the literature. We could loosely define as *kernel* the leftover once a spark has stopped delivering energy and in this paper we focus on the fluid mechanical rather than the very quick plasma-related timescales. This kernel would normally be small, of the order of the spark size. The flame growth would normally occur over lengthscales of the order of the integral lengthscale and

over timescales comparable to some bulk flow timescale. The third phase, full burner ignition, is obviously specific to each geometry studied, but due to the predominance of recirculation zones in most combustors of practical interest, this configuration must specifically be considered. The first two phases, in the specific context of sprays, are discussed in this review separately, to the extent possible. The third phase has received special attention recently from the perspective of ignition probability in flames stabilised by recirculation zones [3, 4] and is also discussed. There is a fourth phase, called *light-round*, that focuses on the flame propagation from burner to burner and is important for gas turbines with annular combustion chambers. This phase is quite configuration-specific and is discussed very briefly in Section 4. The three phases mentioned above are present in all flame types (premixed, non-premixed, spray, swirl *vs.* no swirl, etc.). Due to the turbulent nature of the flows considered, the flow, mixing, and spray patterns at the locality and instant of the spark will be different at different realisations (e.g. at different spark events), and so we may expect significant variability in the result of individual spark events. The stochastic nature of the ignition process in turbulent burners is therefore important to consider and forms a significant focal point of our discussions.

We begin with a classification of the various configurations and canonical problems that are important to study before we build the full picture of the overall turbulent spray flame ignition. We review some fundamental findings revealed by experiment, DNS, and modelling on forced ignition in turbulent non-premixed systems with gaseous fuels that are needed for understanding spray ignition, focusing on the stochastic behaviour and the range of temporal and spatial scales involved. We continue with the separate discussion of the various phases of kernel generation, flame propagation, and overall flame establishment in spray systems, and we consolidate some of the physics by discussing in Section 4 the particular application of gas turbine relight. Some comments on modelling are included in Section 5.

## 2. Classification and key concepts

### *2.1. Autoignition* vs. *forced ignition, kernel* vs. *flame, and relevant scales*

The canonical problem of autoignition of a single droplet in an infinite, stagnant hot oxidiser has been reviewed by Aggarwal [5], and discussed in the context of mixture fraction space in Ref. [6], while the autoignition of turbulent gaseous non-premixed and spray systems (with less emphasis on the latter) has been reviewed by Mastorakos [1]. *Autoignition* must be distinguished from *forced ignition*: in the former, one or both of the reactants (but usually the oxidiser) are already at a high enough temperature for chemical reactions to proceed. The time of ignition or *ignition delay time* (defined, loosely, as the instant when the temperature rises close to its highest value) and the possibility that autoignition is impeded completely are determined not only by the pressure, the initial temperature, and the relevant chemistry, but also by mixing patterns and scalar gradients and their fluctuations [1].

In the forced ignition case, the initial condition is essentially chemically frozen and it is the deposition of energy and/or radical species that raises the temperature high enough, quickly enough, and in a region wide enough for combustion to begin and provide a self-sustaining flame. The spark (treating it either as a heat source or as a radicals source or both) eventually raises the temperature enough for autoignition to proceed; the corresponding ignition delay time is usually very fast or comparable to the spark timescale. Sometimes, failure to ignite can be traced to the slowness of this autoignition process, for instance if the temperature was not raised high enough in case, for example, of a weak spark, or if a substantial portion of the spark's heat is removed by stretch, as through intense turbulence or a very small spark. Let's call this the *first* or *short mode of ignition failure*.

Very often in applications sparks are large and powerful and succeed to initiate a kernel. Perhaps therefore more relevant to practice is the failure to ignite (in a full-burner sense) because a self-sustaining propagating flame cannot be established due to excessive heat loss (e.g. to the evaporating droplets or to the surrounding cold fluid) and/or due to aerodynamic quenching and/or due to fuel starvation (e.g. due to very slowly evaporating droplets), even if a kernel has been generated. Let's call this the *second* or *long mode of ignition failure*. Both these modes of failure have been visualised and explored in gaseous non-premixed systems and sprays by laminar flame simulations [7, 8], DNS [9, 10, 11, 12, 13], and experiments in simplified geometries with methane and liquid fuels [14, 3, 15, 16] and in spark-ignition

direct-injection engines [17, 18] where the second failure mode was deemed to be responsible for misfires.

There is a *third mode of ignition failure*, where the flame grows, fills the combustor, but then extinguishes. This is likely to be related to the phenomenon of blow-off and seems specific to recirculating flames [3, 16]. It may have to do with the fuel accumulation in the combustor during the ignition transient and the failure to create fully-burnt products inside the whole recirculation zone that is the key to stabilisation [19, 20, 2, 21, 22]. This mode is not discussed in this paper.

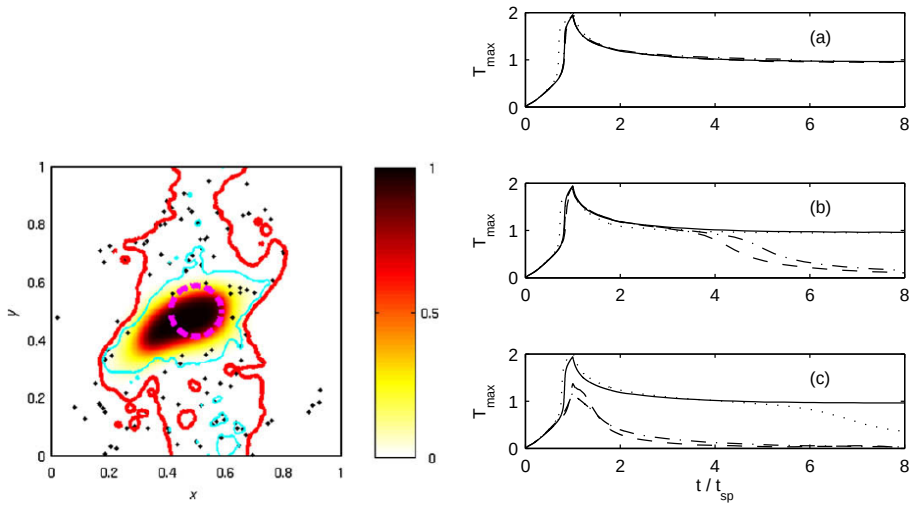


Figure 1: DNS results with 1-step chemistry, point source approximation for the droplets, power source in the energy equation to mimic the spark, and homogeneous isotropic decaying turbulence. Left: Image shows a slice through the domain at $t = 4t_{sp}$, where $t_{sp}$ is the duration of the numerical spark (i.e. the deposition of energy in the domain marked by the thick dashed magenda line). Dots represent droplets, coloured contours represent temperature normalised by the adiabatic flame temperature of the stoichiometric gaseous flame, thick red line is the stoichiometric mixture fraction $\xi_{st}$ and thin blue line $4/3\xi_{st}$. This is a successful ignition event (both kernel and flame propagation). From [12]. Right: Maximum temperature across the whole DNS domain for various cases with different initial droplet size, overall equivalence ratio, and turbulence intensity that demonstrates a different behaviour depending on the value of these parameters. Curves in (a) refer to successful ignitions, (b) to the second (long) failure mode, and (c) to the first (short) failure mode, as discussed in the text. From [13]. Reproduced with permission from Elsevier.

Figure 1 shows the temperature at a time instant following the end of

energy deposition in a DNS calculation [12, 13]. This DNS is with 1-step chemistry and homogeneous isotropic decaying turbulence, and the spray is treated in a Lagrangian manner within the point source approximation (i.e. each droplet contributes to sources of mass, energy, and momentum in the gaseous governing equations) and so the immediate vicinity of the droplet is not resolved. It is important to note that the lack of resolution of the droplet-scale mixing pattern means that such DNS is only an approximation to the true problem. The droplets are uniformly dispersed in a layer of air that is surrounded by layers of unladen air so that no droplets reach the domain boundaries, which was needed for numerical reasons. Attention is given only up to times when the flame propagates in the uniform dispersion.

A successful ignition results in a high temperature region that grows beyond the spark; at the instant shown the flame has outgrown the initial kernel that is approximately equal to the spark for fully homogeneous mixtures, but could be of different size if the spark samples fluids of variable composition. Although initially there was no fuel vapour, in the conditions chosen for this particular simulation there is naturally some evaporation that creates some vapour. But the energy from the spark raised the air temperature further, and this provided heat to the droplets to accelerate the evaporation process. The vapour/air mixture subsequently ignited as the temperature was being raised by action of the spark. Clearly, the ignition timing relative to the spark initiation will depend on the spark power, the thermophysical properties of the fluids, and the number density, size, and volatility of the droplets. In the presence of turbulence, as in the DNS image shown in Fig. 1, it will additionally depend on the turbulent velocity and lengthscale that causes extra diffusion of the spark's heat and mixing of the vapour compared to a quiescent flow.

The evolution of the maximum temperature over the whole domain can be used to reveal ignition success or failure. Looking at Fig. 1 (right), as the spark deposits energy the temperature in the spark region rises above the initial value in an almost linear manner (since the power is constant in this simulation). At some point, the sparked region begins to burn and the maximum temperature rises very quickly to high values; this value could be higher than the adiabatic flame temperature of the stoichiometric gaseous mixture, $T_{ad,st}$, due to the high pre-combustion temperature reached by the energy deposition. When the energy deposition is switched off, the maximum temperature begins to drop and various things may happen, depending on the initial droplet size, overall (liquid plus fuel) equivalence ratio $\phi_0$, and

turbulence characteristics. $T_{max}$ may settle to a value close to $T_{ad,st}$, which corresponds to a successful ignition event: both a kernel was generated (at the spark scale) *and* a self-sustaining propagating flame was created. In some cases (graph (c)), $T_{max}$ very quickly drops back to the initial cold value; this corresponds to the first failure mode, while in others (graph (b)) the flame slowly extinguishes at a time long relative to the spark time. This may correspond to the second failure mode. Wandel [13] correlates the success or failure of the kernel through various quantities that will be discussed later. These possibilities are here shown for sprays, but have also been observed in DNS of gaseous-fuel configurations [9, 10, 11].

For fully premixed systems, the possibility that a flame may fail much later than the instant the spark has been deactivated has been discussed early on by Bradley and co-workers (see, for instance, Ref. [23] and references therein) who used the term *spark overdrive* to denote situations where the spark energy is so large that combustion is sustained by diffusion from the sparked region for a long time and for unusually long distances from the spark. Therefore, if the energy of the spark is large, final success or failure may need a long time to manifest. The extreme of this behaviour is evident in recent research with very lean premixed jets in large co-flows of fully-burnt products, where combustion is sustained even at unusually high Karlovitz numbers due to the presence of the virtually infinite body of hot products [24, 25]. Such configurations are also used to study autoignition of turbulent sprays [26] with interesting results revealing the flame structure and effects of fuel.

Depending on the nature of the fuel and the mixing pattern in the combustor, the study of the second failure mode involves the canonical problems of flame propagation in turbulent uniform mixtures, in non-uniform mixtures, and in sprays, and the extinction of such flames. Turbulent premixed flame propagation is not covered in this paper, as it has been reviewed often before (e.g. [27]), but turbulent flame propagation in strongly non-premixed systems and in sprays is included in the present review. We make the distinction between systems with large mixture fraction fluctuations, wider than the nominally flammable region, and systems with equivalence ratio fluctuations always within the nominal limits of premixed flame propagation, here called *stratified*, following the discussion in Ref. [1]. Forced ignition of the latter is analysed in Ref. [28], where the effects of the characteristic lengthscale and magnitude of the equivalence ratio inhomogeneity on ignition success and flame evolution are discussed. Attached stratified flames have been reviewed

recently [29]. The forced ignition of the former for gaseous fuels and in the presence of turbulence has been reviewed already [1], but some pertinent comments will be repeated in this paper to benefit the discussion of spray ignition.

Figure 1 helps visualise the various time and length scales of this problem and we borrow below some of the terminology and concepts concerning the scales of spray combustion reviewed by Sanchez et al. [30]. Say that at the instant of the spark initiation, the overall (liquid plus vapour) equivalence ratio is $\phi_0$, the percentage of fuel in the vapour phase is $\Omega$, the spray is monodisperse with initial diameter $d_0$, the air has density $\rho$, the pressure is $P$, the initial (unburnt) air temperature is $T_u$, and the homogeneous isotropic turbulence is characterised by a velocity scale $u'$ and integral lengthscale $L_t$. Take $\Omega = 0$, i.e. no pre-evaporation at $t = 0$, the density of the liquid is $\rho_l$, and there are $n$ droplets per unit volume, homogeneously dispersed. Then, the average distance between droplets will be $l_d = n^{-1/3}$, and the fuel mass loading (i.e. percentage of total fuel mass in a unit mass of air plus fuel mixture) will be $a \approx (4\pi/6)(\rho_l/\rho)(d_0/l_d)^3$ assuming a dilute spray (a very good assumption for combustion applications). For gas turbine relight conditions (say, $P = 0.4$ bar and $T_u = 260$ K), a typical spray may have droplets in the range a few $\mu$m to o(100) $\mu$m. Assuming $u' = 10$ m/s and $L_t = 0.05$ m, values of the right order of magnitude for a gas turbine combustor, gives a Kolmogorov lengthscale $\eta_K$ of about 50 $\mu$m (i.e. of the order of the usual $d_0$) and a large-eddy turnover time $\tau_t$ of 5 ms. An equivalence ratio $\phi_0 = 0.5$ implies $l_d/d_0 \approx 50$, while for $\phi_0 = 1$ and 10, $l_d/d_0 \approx 40$ and 20 respectively. Therefore the average inter-droplet distance is, for most practical applications, large compared to the droplet size. In the absence of spark and for a fuel with low volatility like kerosene, the time for complete evaporation of the droplet, $\tau_{evap}(T_u)$, will be large compared to the residence time in the combustor and the large-eddy turnover time. But if a spark lasting $\tau_{sp}$ and acting in a volume with characteristic size $d_{sp}$ results in raising the temperature in that region to $T_{sp}$, the evaporation time $\tau_{evap}(T_{sp})$ will be quicker. Estimates of the evaporation time of single droplets of kerosene surrogate at relight conditions can be made by codes similar to Ref. [6]. Hence, at $T_{sp} = 2000$ K, $\tau_{evap}$ for a 20 $\mu$m droplet is about 3 ms while for a 100 $\mu$m droplet it is about 75 ms, the autoignition time is about 0.5 and 2 ms, and the burnout time of an envelope droplet-scale flame is 1 and 15 ms respectively (A. Giusti, personal communication). It is conceivable that droplet-scale flames are indeed ignited inside the kernel in gas turbine relight

problems because the autoignition time of an isolated droplet in the hot air is short. However, we should note that the behaviour of a spray inside the plasma from a powerful spark is not known at present and hence equilibrium evaporation models may be in large error.

The ratio $\tau_{evap}/\tau_{sp}$ affects the amount of fuel vapour that will be generated by the spark while the ratio $\tau_{sp}/\tau_t$ can determine whether turbulent mixing will stretch the sparked region and hence introduce significant heat losses. In terms of lengthscales, $d_{sp}/l_d$ and $l_d/L_t$ seem appropriate ratios to consider. Electrical sparks may last of the order of a ms (e.g. [17, 18, 14]). Laser sparks deliver energy over only a few ns, but once the plasma has cooled to, say, 3000-4000 K, a time period of the order of hundreds of $\mu$s may have elapsed [31, 32]. Normally sparks are not too small and tend to be of the order of the electrode gap in automotive applications (e.g. [18]) or even many centimetres in size in gas turbine applications [33, 34, 35], which implies that the characteristic lengthscale of the spark lies closer to the turbulent integral lengthscale than the Kolmogorov lengthscale. Probably we cannot treat sparks as points in the turbulent flow. The DNS data shown previously in Fig. 1 reveal that, for a given spark (size, energy, and duration) and a given thermochemistry, the value of these ratios can have a direct effect on the success of the ignition and also determine the mode of failure. It has often been demonstrated with such DNS that too small sparks result in failure (e.g. Ref. [36]).

### *2.2. Stochasticity*

A very important point concerning spark ignition of all combustion systems, but more so when one considers non-premixed and spray flames and when one is focusing on the whole flame establishment, is the fact that all the individual processes leading to whole flame ignition involve stochasticity [1]. Therefore, each spark event may lead to a different behaviour. In quiescent, homogeneous premixed systems, this is due to the spark itself because the ionisation path is not identical every time a spark is created between two electrodes. A spray, even without turbulence, will have mixture inhomogeneities across the spark volume due to the random droplet spacing and hence even if the energy deposited to the fluid and the shape of the spark were identical in every spark event, the ignition process can be different. A turbulent non-premixed system will involve fluctuations of the strain rate and the mixture fraction and so the probability of establishing a kernel, $P_{ker}$, is an important quantity to consider [1]. The subsequent phase of flame evolution and

burner ignition may introduce extra fluctuations due to the various possibilities associated with the flame motion following a spark. Hence, the flame may quench or grow, and the whole burner may ignite or the flame may be blown away. These behaviours have been visualised and analysed in a range of geometric configurations such as an axisymmetric jet [14, 37], counterflow [15], and bluff-body non-premixed flames [3], and it has been found that the difference between the measured $P_{ign}$ and $P_{ker}$ are significant. Individual successful and failed ignitions (misfires) in a spark-ignition engine have also been analysed from the perspective of instantaneous conditions at the spark [18]. Similarly in fully premixed recirculating flames, even if locally a kernel is created, not all locations result in full flame establishment (i.e. $P_{ign} < 1$) [38, 39, 40]. In spray flames, these probabilities have not been measured as extensively as in gaseous systems. Marchione et al. [4] measured $P_{ign}$ in a heptane swirling flame and found strong spatial variations of $P_{ign}$ that can help understand what spark locations are more likely to result in successful overall ignition. The factors that affect $P_{ker}$ and $P_{ign}$ are discussed in the context of the separate ignition phases in Section 3 and in the context of more complex but realistic gas turbine combustors in Section 4.

### *2.3. Configurations studied*

The literature contains many experiments and simulations on a range of simplified (canonical) problems, some of which are given in Fig. 2. The spark in a uniform dispersion, which gives rise to a spherically-expanding flame, is one of the building blocks for our understanding. The conditions of ignition that give rise to a self-sustaining flame and the speed of this flame are the key topics of interest. There is also the situation of sparking somewhere across a mixing layer between a droplet-carrying stream and droplet-free air; this layer could be strained or not and could be turbulent. Parts of the flame will evolve as an edge flame, which is a topic that is important for the overall ignition of a spray flame. The canonical problem of (nominally planar) laminar and turbulent flame propagation in a gas carrying a droplet dispersion must also be considered.

Finally, sparking and subsequent flame evolution and full burner ignition in swirl flames has been recently studied due to the practical relevance of this configuration. These problems have their gaseous counterparts, most of which are reviewed in Ref. [1]. It may be surprising that forced ignition in spray jet flames has not been performed yet, despite the apparent simplicity of this geometry and its proven usefulness for gaseous non-premixed and

spray combustion research (for an entry to the recent literature on spray jet flames, see Refs. [41, 42, 43]).

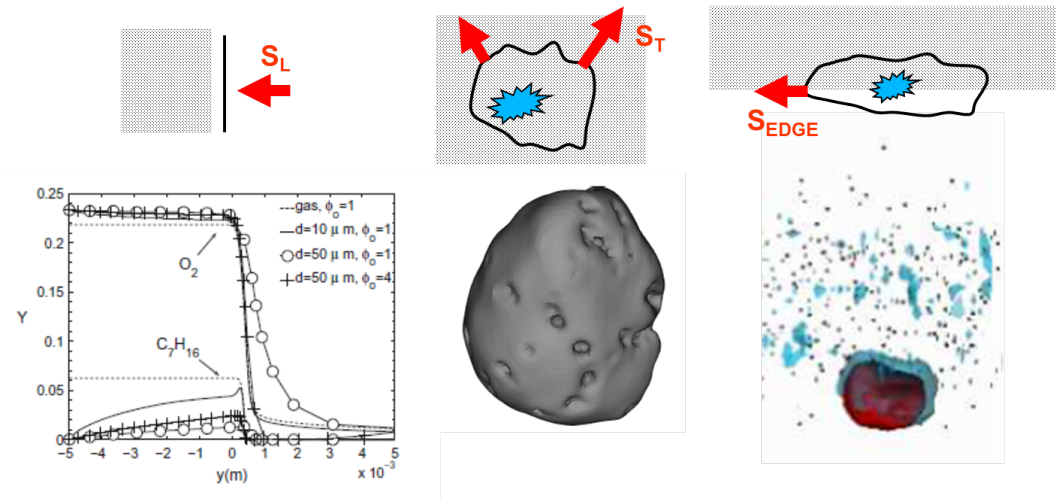


Figure 2: Canonical configurations for understanding full ignition of a combustor and some representative simulation results for illustrating some key findings. Upper row of sketches schematically show the configuration, with shaded area indicating the droplet dispersion. Lower row is from simulation results. Left: Laminar planar flame propagation in a uniform dispersion of droplets. The lower figure is from Ref. [44] and shows the flame structure from 1-D flame simulations. The turbulent version of this configuration has been studied very little, but experimental [45] and DNS studies [46] begin to appear. Centre: Spark ignition in a uniform mist. The lower figure is from DNS [47] and shows that the iso-surface of $T = 1400$ K includes turbulent but also droplet-scale wrinkling. Although this configuration has been studied experimentally without turbulence, there is very little work with turbulence. Right: Edge flame propagating in a region with $\phi_0$ inhomogeneity, a situation that has not been studied by experiment yet. The lower figure is from DNS with one-step chemistry [36], that shows a flame kernel (red) expanding towards the spray; blue is the isosurface where the gaseous mixture fraction is stoichiometric. Clearly, the flame generates its own vapour. Reproduced with permission from Elsevier.

## 3. The phases of ignition

### *3.1. Phase 1: kernel generation*

The initiation of a flame through a spark in a flammable mixture is one of the fundamental problems in combustion and has been studied very thoroughly from the perspective of conditions that allow an embryonic kernel may grow. Usually, the spark itself is not considered. Standard combustion textbooks contain significant details on this problem, from both a theoretical and an experimental viewpoint [48, 20, 19, 2]. A large effort has also been devoted to the effects of flow, and of the turbulence in particular, on the success of ignition. This work has shown, in general terms, that to ignite a flammable mixture one needs to deliver enough energy to raise a region of characteristic size proportional to the laminar flame thickness (the quenching distance, to be more exact) to the adiabatic flame temperature [19] and that the presence of turbulence can be detrimental to ignition due to straining of the flame kernel that may hence be extinguished [2, 23, 49]. This energy is called the Minimum Ignition Energy (MIE).

It is important to remember that many of the experiments that measured the MIE did so through a direct quantification of the stochasticity of the process. The usual procedure is to deliver a given (nominal) energy, $E_{sp}$, a number of times and count how many times a flame was successful (see, for example, recent such experiments on laser ignition of n-decane at a range of conditions [50] where particular emphasis is placed on the ignition probability). This is the $P_{ker}$ we have introduced previously. As $E_{sp}$ increases, $P_{ker}$ increases from zero and eventually reaches unity (i.e. all sparks produce a kernel). The MIE is usually defined as the energy such that 50% of the spark events result in flame. In the presence of turbulence, the fluctuations of the local strain rate can reduce $P_{ker}$ in all combustion systems (premixed, non-premixed, spray) [51]. Therefore, even the well-studied "textbook" concept of MIE involves some vagueness and randomness and needs careful definition. This can be important for safety studies [52] and considerations concerning the certainty of ignition, which are necessary concerning spark-ignition engine misfires and jet engine high-altitude relight.

The spark itself is often not considered in theoretical analyses, but recently some work with simulations including the plasma and with imaging at timescales close to those of the spark has been performed that highlights some important features. First, for electrical sparks that tend to be long-lasting (i.e. of the order of tens or hundreds of $\mu$s or even ms), the spark

and the ignited kernel may be severely stretched by the flow [18, 4, 53, 54]. This allows the possibility that the kernel may encounter conditions more conducive to propagation or quenching at localities away from the nominal sparked region and this is important to consider for the correct placement of the spark, e.g. relative to the recirculation zone in swirl flames [4], and for modelling of flame evolution in engines [54]. For laser sparks that are very short (a few ns), the breakdown provides a plasma of characteristic size of a few mm (e.g. [55]). The various species contained in this plasma have very different timescales. Hence, atomic species like H, O, and N have a lifetime of 1-2 $\mu$s [55, 32, 31], while longer-lived molecular species CN and $C_2$ may survive at the timescale of order 0.1 ms (M. Kotzagianni, unpublished). It is not clear which of these contributes, in a chemical sense, to promote combustion in the kernel; compound plasma and combustion chemistry mechanisms such as those in Refs. [56, 57] are needed to explore this.

Following the sudden deposition of energy and the combustion at the kernel, a shock wave may emanate from the spark (see, for instance, Ref. [31] and references on laser ignition therein). This shock wave is not strong enough to compress the mixture and cause autoignition, but it is sufficient to trigger droplet oscillations and break-up [58]. For gas turbine relight, this may be especially important because the poor atomisation associated with the low flow rate and gas density at the air-blast atomiser at an engine flameout would make ignition and flame propagation difficult, but this mechanism promotes the generation of fine droplets and subsequent evaporation. Simulations of the interactions between plasma and the initiation of combustion chemistry in flammable mixtures begin to appear [57, 56] and the spark stretching and growth has been simulated by LES [53] at the $\mu$s timescale. No such calculations are available at present for sprays. The interaction between arcs, discharges, and all kinds of plasma with droplets and fluid sheets and ligaments is very poorly studied at present; more work is needed in this area in order to understand the short timescale phenomena associated with the first phase of ignition in a spray.

In a realistic combustor the flow is turbulent and the droplets are not uniformly dispersed and hence the presence of equivalence ratio local inhomogeneities must be taken into account. Therefore, the fundamental problem of kernel generation in a turbulent non-premixed flow must be studied. Let us first consider gaseous fuels. Work with laminar diffusion flame simulations [7], Direct Numerical Simulations of turbulent mixing layers [59, 60, 10], and experiments [14, 15, 3] has demonstrated that spark-ignition of turbulent

non-premixed combustion has a stochastic nature, as discussed before, with the randomness arising through the mixture fraction fluctuations, as first suggested by [61], and additionally through the velocity fluctuations at the spark location [14]. In particular, it has been found that the stochastic nature of ignition, given energy deposition at an instant and at a point in a turbulent flow, can be discussed through three, separate, probabilities. First, the probability of finding flammable mixture at the spark, denoted as *flammability factor* and defined as [61]

$$F = \int_{\xi_{lean}}^{\xi_{rich}} P(\eta) d(\eta) \tag{1}$$

where $\xi_{lean}$ is the nominal lean flammability limit expressed in terms of the mixture fraction $\xi$, $\xi_{rich}$ is the rich flammability limit, and $P(\eta)$ the probability density function of the mixture fraction. Second, the probability of generating a kernel, $P_{ker}$, determined for example, by depositing many times the same amount of energy in the flow and measuring the percentage of events resulting in successful kernel generation. Finally, the probability of whole-flame ignition, $P_{ign}$, is the probability that the spark will generate a kernel, and the kernel will grow to ignite the whole flame. The difference between $P_{ker}$ and $P_{ign}$ is very important, as already discussed, and will be discussed again in the next sub-section because this quantifies the success of the second and third phases of ignition.

The difference between $P_{ker}$ and $F$ is important and interesting. Experiments show that $P_{ker}$ is not always equal to $F$ [3, 15]. The possibility that $P_{ker} < F$ may be expected: intense strain rate or scalar gradients at the spark location can quench the kernel. Therefore, even if a spark sampled flammable mixture, the kernel may immediately get quenched. Simulations in laminar non-premixed flames show that the critical strain rate above which ignition can fail is *lower* than the extinction strain rate of an established diffusion flame [7] and that this critical strain rate for successful ignition depends on the location of the spark. The simulations also demonstrate long-range effects, where, despite the fact that the spark may be located outside the nominally flammable region, enough heat is diffused to the flammable region to cause ignition there. In a turbulent flow, this is translated as $P_{ker}$ (and perhaps $P_{ign}$) being finite at a location where $F$ is zero. This prediction has been confirmed by experiment. For instance, in Ref. [15] in a turbulent counterflow non-premixed configuration (methane impinging on air), spark-

ing deep into either of the two streams and away from the mixing layer could still result in ignition because the predominant convection brought the hot gases from the spark to the mixing layer and hence in contact with flammable material. Similarly, in the axisymmetric jet, sparking fluid beyond the nominal flammability limits could still result in ignition [37]. It is interesting that despite the fundamental nature of this problem, very little work has been done on spark ignition of laminar non-premixed flames.

In the context of igniting a spray flame, these findings must be extended to include the presence of liquid droplets. From the point of view of the MIE required to initiate a kernel, there is extra energy needed to evaporate the fuel [62, 63, 64, 65, 66, 67, 68]. The minimum ignition energy decreased with decreasing droplet diameter, increasing fuel volatility, and with an increase in fuel vapour content in the droplet-air mixture [69, 51]. In addition, extension of the lean ignition limit was observed, attributed to droplet evaporation creating inter-droplet regions of gas-phase equivalence ratio more favourable to ignition than the overall equivalence ratio [64]. The review by Aggarwal [70] discusses trends from various sources and in particular from the work of Ballal and Lefebvre that showed that the minimum ignition energy of a droplet-laden turbulent air flow, with the droplets relatively uniformly dispersed, increases over the value expected from ignition of a gaseous-air mixture of the same total equivalence ratio due to the energy necessary to evaporate the droplets [2, 71, 72, 73, 51]. The droplet parameters (size, number density) affect MIE in a complicated manner, which can approximately be correlated by stating that the ignition energy will be minimum when the vapour created will be close to stoichiometric. In the case of turbulent dispersions, the presence of turbulence increases the minimum ignition energy [51].

In addition to the energy, the timescales of the problem are also important. Ballal and Lefebvre [51] reviewed their previous work and correlations and proposed that for a successful kernel (i.e. for the kernel to grow) "*the time required for the fuel to evaporate and burn must be equal to, or less than, the time required for the cold mixture to quench the spark kernel by thermal conduction and turbulent diffusion*". This concept required an estimation of the individual processes, which involves various approximations, nevertheless it included all known effects of droplet size, equivalence ratio, degree of prevaporisation, turbulent intensity, and kinetics (the latter through the flame speed of the gaseous flame). The model has a reasonable degree of success to collapse available data on MIE from dispersions. More refined theoretical

descriptions of this early phase of ignition in sprays are currently underway [74].

Therefore, the physical reasons why the MIE needed to ignite a spray can be different than the MIE needed to ignite a gas can be summarised as follows. First, extra energy is needed for evaporation. Second, the vapour content is variable in time and space and is affected by the progress of the reaction. Third, the droplet evaporation timescale acts additionally to the chemical timescale and the diffusion timescales to determine the overall rate of the process and may compete with the chemistry, which can lead to flame extinction if the spray does not evaporate quickly enough. Finally, the turbulence will affect the process in a broadly similar way it affects the survival of an ignition kernel in fully premixed systems.

The stochastic nature of spray ignition has so far been studied only in the context of the equivalence ratio fluctuations at the droplet scale in laminar flow (see, for example, Ref. [70]), rather than in the context of the large-scale inhomogeneities found in a spray flame as in a jet (e.g. [43]) or a swirl combustor. Both are expected to be present when igniting a realistic turbulent spray, with the latter probably dominating for turbulent flows. Further work is needed to understand the distribution of $P_{ker}$ in sprays.

Recently, Direct Numerical Simulations of spark ignition in a spray with simplified chemistry [12, 36] and complex chemistry [47] have revealed some features on the micro-structure of the flame in its initial stages, its propagation mechanism, and conditions at which the ignition may fail. We repeat that such DNS research has limitations because the droplet-scale fuel distribution is not accurately resolved. Nevertheless, interesting insights can be achieved. Figure 3, taken from [47], shows that the deposition of heat in a volume inside the spray (visualized in the figure with the grey surface that marks the iso-surface of temperature being equal to 1400 K) results in localised ignition of individual droplets, with the reaction proceeding first with endothermic, pyrolysis reactions and then with strongly exothermic combustion. The individual droplet-scale flames that first ignite eventually merge to give rise to a very distorted and highly-curved flame sheet, where the reaction proceeds at a wide range of mixture fractions [47]. Interestingly, for some time and due to the spark's energy, mixture fractions way outside the nominal flammability limits also show finite reaction rate, which is another manifestation of the "spark overdrive" effect mentioned previously.

Some of the extensive wrinkling shown in Fig. 3, also evident in Fig. 2 (centre, lower) for a case with $\phi = 8$, would also be present in the absence of

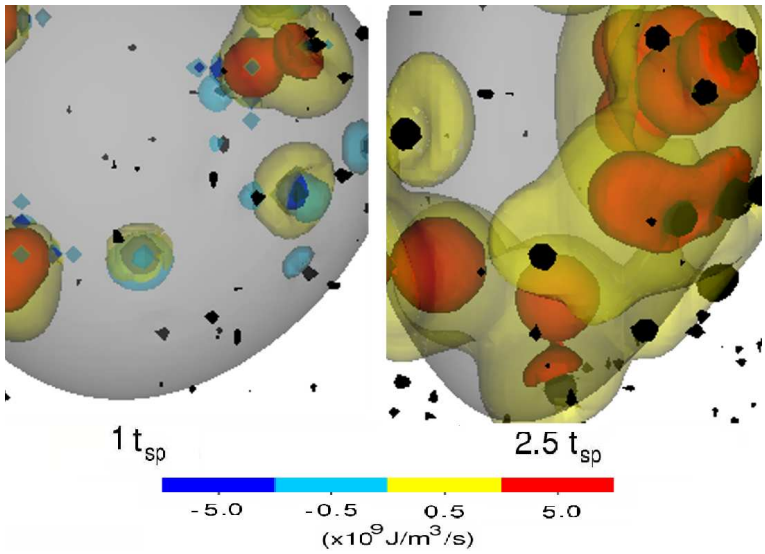


Figure 3: DNS of forced ignition in a uniform dispersion of 20 $\mu$m n-heptane droplets, $\phi_0 = 1$, in air at atmospheric conditions and with homogeneous isotropic decaying turbulence. Coloured iso-surfaces of heat release rate during at two different times ($t_{sp}$ denotes the duration of the spark). The temperature iso-surface $T = 1400$K is in grey while the stoichiometric mixture fraction iso-surfaces $\xi = \xi_{st}$ are shown in black (can be thought of as surrounding individual droplets). Droplet-scale combustion is evident in the beginning, giving rise to a connected reaction sheet later. There is severe local wrinkling due to the mixture fraction inhomogeneity in the inter-droplet space. From [47]. Reproduced with permission from Elsevier.

turbulence, since it is associated with the inhomogeneity associated with the random location of the droplets. Models including this source of curvature to the usual wrinkling mechanisms due to turbulence would be needed for a correct theoretical treatment of turbulent flame propagation in sprays. It is also evident that such models must include the possibility of stratified premixed and conventional non-premixed combustion.

Simulations [47] also show that very rich flames, for example with overall equivalence ratio of 8, can still ignite successfully due to the fact that in the inter-droplet region equivalence ratio regions closer to stoichiometry can always be found as vapour is generated by the action of heat transfer from the spark. This is relevant to gas turbine ignition that often involves sparking in very rich regions, for example in fuel-flooded surface discharge igniters.

An attempt to identify the exact conditions leading to short failure mode

(i.e. immediately after the spark ends), to long failure mode (i.e. much later), and to successful propagation in a spray has been made by exploring one-step chemistry DNS data [13]. The key seems to be the presence of incompletely combusted fuel at the instant the spark energy deposition stops. If this happens, then the kernel will eventually fail. But if the progress variable is high across a substantial volume so that the spatial gradient of the progress variable is small, then success is likely. Important quantities are the PDF of the progress variable and its dissipation rate and the cross-dissipation between oxygen and fuel vapour. Similar simulations with detailed chemistry are necessary in order to consolidate these interesting suggestions.

### *3.2. Phase 2: flame growth*

Successful ignition of a combustor involves not only the successful generation of a flame kernel following the energy deposition by the spark, but also flame propagation and overall stability of the flame.

For gaseous fuels, some results focused on this topic have begun to appear. For example, [3] recently visualized ignition in swirling and non-swirling recirculating methane flames by a single spark and the spatial distribution of the ignition probability $P_{ign}$ ("ignition" defined as the overall successful flame establishment) showed quite unexpected shapes, which could be understood through local mixture fraction and velocity measurements. An interesting finding was that under some conditions, despite the fact that the recirculation zone was mostly flammable, sparking there did not result in overall flame ignition due to localised quenching. Sometimes, however, ignition was possible. The results were interpreted in terms of the local Karlovitz number, which nevertheless has not been the sole factor determining burner ignition even in fully premixed systems [40, 38].

It was also demonstrated that regions with high ignition probability are those where the mean mixture is not far from the stoichiometric, the flow velocity is favourable for upstream flame propagation, and the local turbulence weak enough or the mixture strong enough so that the small flame kernels initiated from the spark are not extinguished. In jets [14, 75], ignition must be provided up to a particular distance from the nozzle if the flame is to travel back successfully. The speed at which the flame travels back is an important target quantity for validation of models [76, 77].

Non-local effects have also been observed [15, 3, 37] where $P_{ign}$ can be finite in regions where $F \approx 0$, as discussed before. Data by Ahmed et al. [3] show large differences between the measured $P_{ign}$, the measured $F$, and

$P_{ker}$. Such non-local effects have also been examined by simulations [7, 10] that demonstrated that the local value of the mixture fraction at the spark location is not sufficient to explain ignition behaviour.

Once a kernel has been generated, and a sizeable flame around the stoichiometric mixture fraction isosurface has been created, the flame may then propagate along this isosurface as a non-premixed edge flame [1]. This structure has been quite obvious in laminar jets [78] and by OH-PLIF images in situations with large mixture fraction fluctuations, such as in the turbulent counterflow [15]. When the kernel is in regions of the flow with small mixture fraction fluctuations, such as in the centre of a well-mixed recirculation zone, the flame propagates initially as a premixed or stratified flame [3, 1]. Failure to propagate in either premixed or edge flame mode results in a reduced $P_{ign}$. Non-premixed edge flames have received significant attention for laminar flows [79, 80, 81], but have been relatively little studied in the presence of turbulence and their extinction behaviour is not very well understood. Refs. [59, 60, 82, 83] provide data from simulations and experiments for the average edge flame propagation speed in igniting turbulent mixing layers and it is shown that the average displacement speed (i.e. the propagation relative to the local fluid ahead of the flame) is only a fraction of the laminar burning velocity of an unstrained premixed flame and that intense turbulence is detrimental for this speed. The DNS [83] and the experimental [82] PDFs of displacement speed are in remarkable agreement. The relatively slow displacement speed of the flame edge following spark ignition in fuel-air mixing layers has been attributed to the turbulent strain.

Significant additional complications are found in flame propagation in sprays. The first canonical problem to consider is the spherically-growing flame in a uniformly-dispersed droplet-air mixture (e.g. Fig. 2, centre). The Introduction in the paper by Greenberg [84] serves as a very good overview of this problem for laminar systems. The literature review by Neophytou et al. [36, 47] may also be a good start. We mention here a few trends from experiments [85, 86, 87]. In general, the propagation speed is a strong function of droplet size, overall (liquid plus vapour) equivalence ratio $\phi_0$, and degree of pre-evaporation $\Omega$. First, the presence of droplets generally cause a reduction in the flame speed relative to the flame speed of the fully prevaporised case (i.e. at the same equivalence ratio). This is mostly attributed to the time needed for evaporation [85]. Second, the presence of stretch in the spherically-expanding flame may lead to significant alterations of the flame speed and even quenching [88]. A related finding from analytical work

is that the extinction strain rate in counterflow spray flames shows a severe reduction compared to the gaseous flame value, mainly due to the finite time needed for evaporation [89, 90] and that the polydispersity of the spray is important to consider (describing the spray only through the usual Sauter Mean Diameter is not sufficient) [91]. Third, large droplets result in a decrease in flame speed [85]. Fourth, a very rich mixture may result in a surprisingly high flame speed due to the fact that the equivalence ratio the reaction zone "sees" can be smaller than $\phi_0$ and may hence approach stoichiometry. But an additional reason given for this trend is the droplet-scale flame wrinkling and local mixture inhomogeneities that may introduce stoichiometric mixture "bridges" between the droplets, for example as seen in both simple-chemistry [92] and complex chemistry simulations [47]. See also Fig. 3. Neophytou et al. [47] suggest that this mode of flame propagation is related to the spray's Group number. This propagation mechanism through the inter-droplet region is roughly equivalent to the suggestion that the flame travels through igniting droplet-scale flames as the front jumps from droplet to droplet and has received significant attention with experiments with droplet lattices. For example, Niioka [93] concluded that the maximum flame speed is found at a droplet spacing around 1/2 of the diameter of a single-droplet flame; if the latter is around 5-6 times the droplet diameter (from the experimental data of Ref. [93] and consistent with single-droplet simulations [6]), the maximum flame velocity in Niioka's experiments occurs at a very rich $\phi_0$.

Recent analytical work [94] has also provided insights into the reasons why the global stoichiometry affects the flame speed and the MIE, and also demonstrate the possibility of extinction due to stretch. The MIE and flame speed in mists has also been discussed from the perspective of explosions [52], which provides an additional focused review of the literature of this problem. However, very little work has been done with a focus on turbulence effects on the spherical flame expansion process. There is mention of high turbulent intensity experiments in large-scale explosion vessels, which show very high flame speeds, but the details given are not sufficient to build a complete picture [95].

Simulations of laminar planar one-dimensional freely-propagating flames in spray mists with detailed chemistry [44] (see Fig. 2, left) have replicated many of the above experimental trends and have provided some support to the model of Ballal and Lefebvre [85], which provides an estimate of the flame speed in sprays as a function of the spray characteristics (SMD, volatility, $\phi_0$, $\Omega$) and the fuel characteristics ($S_L$) by looking at the chemical and the

evaporation timescales. The delay associated with evaporation causes the equivalence ratio at the reaction zone (called *effective equivalence ratio*) to be less than the global, nominal one. This is evident in Fig. 2 (left, lower), taken from Ref. [44], where the fuel mass fraction in the pre-flame region is shown for various conditions (droplet size and $\phi_0$). For lean $\phi_0$ this causes a reduction of the flame speed. But for rich $\phi_0$ and for large droplets, the effective equivalence ratio may approach stoichiometry and the speed can be high. Even for $\phi_0$ much richer than the rich flammability limit, the simulations show a substantial flame speed. (These calculations will also be discussed in Section 4 as they can be used to provide estimates of flame speed for relight conditions.) Additional complexities of a chemical nature have also been revealed [44], which were not present in one-step chemistry modelling efforts. For overall rich sprays and for droplets that are not too small, the post-flame evaporation of surviving droplet results in fuel release into a hot oxygen-free environment. This leads to pyrolysis, which results in hydrogen and acetylene generation that can then increase the flame speed by diffusing back towards the reaction zone [44]. The flame acceleration may be substantial.

The fact that very rich sprays and with large droplets can still show finite flame speed may have an important implication in ignition of realistic burners. Usually, gas turbine ignitors deposit very large amounts of energy, which can evaporate and ignite everything in the spark's vicinity. Burner ignition failure is then a matter of flame propagation failure. But burner ignition success may be unexpected considering the richness of the spray in the spark location. The above argument that explains the relatively high flame speeds in laminar rich sprays suggests that overall rich locations in a spray combustor may end up having significant flame speeds and hence promote ignition.

Experiments with turbulent planar spray flames in homogeneous (in the mean) dispersions, our second canonical problem, are quite limited. The work of Lefebvre and co-workers, with a flowing uniform droplet dispersion and V-shaped flames stabilised on a central torch [85, 96, 97], has shown flame speed trends similar to the ones with the spherically-expanding flames, but also highlighted some complexities associated with ensuring uniformly-dispersed droplets (and hence homogeneous $\phi_0$) and with the estimation of $\Omega$ (measuring $\Omega$ directly is very difficult at present), that may make some quantitative results difficult to interpret [97]. Note also that in most of the spherically-expanding flame experiments the mist was created by condensa-

tion of a super-heated vapour and hence the droplets were usually relatively small (say, in the range 5-20$\mu$m [86, 98]), but in experiments with flow the spray is created by atomisers and hence we expect larger droplets sizes and significant polydispersity. Therefore, the available experiments with turbulent flames in a uniform dispersion of droplets are not sufficient to build a complete picture of the phenomena. A cone-shaped turbulent flame stabilised on a Bunsen burner [45], with the fuel (n-heptane) provided in droplet form carried by the air, has been explored in terms of mean progress variable distributions for various spray parameters and in terms of mean evaporation rates and how these are affected by the flame. However, further information such as turbulent burning rate, local displacement speed, curvature statistics and other quantities that are used often in the description of turbulent premixed flames is not available. Simulations of this problem are also very limited. Recent DNS of turbulent flame propagation in droplet mists [46] have revealed severe equivalence ratio fluctuations along the flame front, droplets surviving the flame, and a burning rate reduced over the gaseous one.

The literature on turbulent flame propagation in sprays is very sparse. This area needs significant further work before solid conclusions can be made. Due to the very inhomogeneous mixtures formed in the inter-droplet spacing, the intense local stretch, and the pyrolysis effects in locally rich regions, using detailed (or anyway, complex-enough) chemistry for spray flame simulations is preferred. More experiments are needed and these must focus on local flame structure, droplet-scale *vs.* cloud combustion, polydispersity, and multi-species measurements among others. The challenges due to the small scales involved are of course enormous.

In a combustor, the droplets are non-uniformly dispersed, giving rise to $\phi_0$ large-scale inhomogeneities and therefore to flame speed variations (see Fig. 2, right). The stable flame in jet spray systems has received attention [43], although spark ignition experiments in these configurations have not been attempted yet. The structure of the leading edge in a lifted spray jet flame has been visualised and, under some conditions, it looks similar to edge flames in gaseous jets although it lacks the three distinct branches visible in triple flames [99]. In an effort to numerically study edge flame propagation in sprays, Neophytou et al. [36] examined spark ignition and subsequent flame propagation in a mixing layer between air and air laden with fuel droplets with DNS. Like in the edge flame in the gaseous mixing layer, the edge flame displacement speed was again only a fraction of the laminar burning velocity of the stoichiometric gaseous fuel, which implies

that the flame spreads mostly by the turbulent motions of the flow. However, finite propagation rates are absolutely necessary in order to maintain the flame alive (i.e. unquenched) as it spreads. This concept is important for modelling burner ignition, as discussed in Section 5. Analytical studies reveal that the edge flame in inhomogeneous spray can extinguish due to strain and that the edge flame propagation speed decreases with decreasing volatility of the fuel [8], predictions that are in agreement with the DNS results in turbulent flows and over a range of spray characteristics [36]. Figure 2 (right, lower) shows that the flame growing along the mixing layer extracts vapour from the spray in the immediate proximity of the flame sheet, making the local equivalence ratio and the displacement speed quite variable. Further simulations (preferrably with detailed chemistry) and experiments in this configuration are needed.

### *3.3. Phase 3: burner ignition*

Assume that energy has been deposited from a spark, a kernel has been generated, and a flame has propagated from the kernel (i.e. the flame has grown). These are necessary conditions for overall combustor ignition, but not sufficient. Overall burner ignition, Phase 3, will happen if the flame moves in the right direction and if the whole flame is stable once ignited.

In a series of focused, fundamental experiments to understand this issue better, swirling and non-swirling flows around axisymmetric bluff bodies with gaseous and liquid flames have been studied [3, 4, 16]. These experiments supplement the large body of work on spark ignition in realistic geometries and conditions that is discussed in Section 4.

In these more academic experiments, a single spark has been deposited many times in various locations and the number of times the burner was ignited was determined. This gave the ignition probability, $P_{ign}$, as a function of location for various flow conditions (such as flow rate, fuel to air ratio, spark energy, spark repetition rate). An important qualitative finding is that $P_{ign}$ changes very steeply from point to point. The original papers explain in detail the reasons for these variations. Visualization shows that successful ignitions are associated with flamelet movement towards the bluff body, i.e. the recirculation zone must capture the flame ensuing from the spark, and recirculate it in order to allow the flame enough time to grow, but also in order to ignite the critical region close to the anchoring point. The direction of the instantaneous velocity in the spark vicinity has also been shown to play a role for successful flame growth and the pressure rise

in a spray-guided spark-ignited direct-injection engine [18], in remarkable similarity to the ignition of recirculating premixed, non-premixed, and spray flames [40, 3, 4].

Not all such ignition events are successful. Some events that seem to have ignited the whole flame surrounding the recirculation zone, and hence would be considered successful ignitions, still fail [3]. This is the third mode of ignition failure, discussed previously. This may have to do with the fact that significant time is taken for the flame to reach the fully burning state and the recirculation zone to become very hot (revealed, for example, by Large Eddy Simulations [100, 101]), and implies that burner ignition occurs over a quite long timescale relative to the spark and the flame propagation timescales. Letty *et al.* report such failures on the order of 100s of milliseconds [16]. Note that these naturally transient experiments offer great opportunities for validating simulation methods.

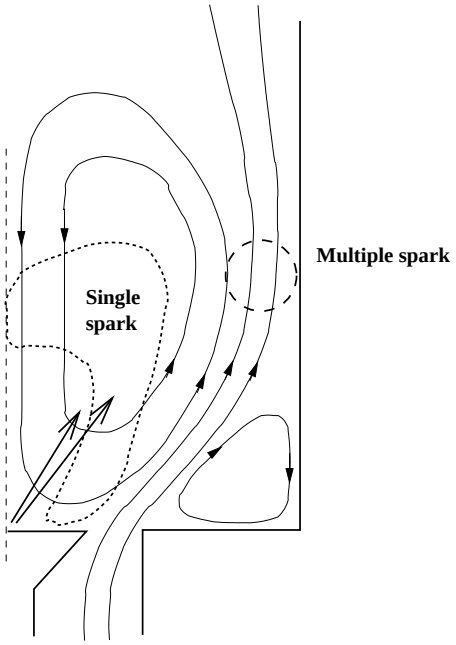


Figure 4: Sketch summarising the best positions for ignition from the single spark (dotted curve) and from a multiple spark (100 Hz; located along the enclosure) (dashed circle) superimposed on a schematic of the air streamlines and the spray trajectory, in a hollow-cone swirling spray flame. From [4]. Reproduced with permission from Elsevier.

The spark ignition of a swirling spray flame of n-heptane [4] has revealed similar trends to those of the non-premixed recirculating flames. Regions giving high $P_{ign}$ were those that had mean $\phi_0$ close to the stoichiometric, with small Sauter Mean Diameter, and with mean axial velocities in the direction of the spray injection point that decreased the likelihood of the flame being convected away. In addition, a series of experiments with multiple sparks placed close to the combustor wall, to mimic the placement of the ignitor in gas turbine combustors, were performed. From these measurements, the most favourable regions for spark ignition have been summarised in Fig. 4 [4]. The best position for ignition with a repeated spark at the wall is at the axial location corresponding to the maximum width of the recirculation zone because this maximises the chance of spark stretching and hence penetration into regions with negative velocity (i.e. towards the root of the spray). Further ignition probability measurements in spray combustors are necessary. Simultaneous imaging of the kernel and the underlying velocity, equivalence ratio, and spray parameters must be performed. Such simultaneous experiments have been performed in an engine [17, 18]; similar quality data are needed also for swirl combustors. Note that the degree of pre-evaporation is very important; it is not clear how this can be measured with the currently available laser diagnostic techniques.

## 4. Application: gas turbine ignition

### *4.1. The problem of ignition at high altitude*

Ignition of a gas turbine combustor is an increasingly important issue for engine manufacturers due to the current trend towards lean operation that makes flame initiation more difficult. In aviation engines in particular, high-altitude relight is a significant problem. Once the engine has extinguished, the temperature and pressure in the combustor are low causing a significant decrease in the vapour pressure of the fuel and the decreased air flow rates may lead to poor atomization, both of which imply the need for large amounts of spark energy to initiate a flame kernel [69, 70] and a lower flame propagation speed [85, 102].

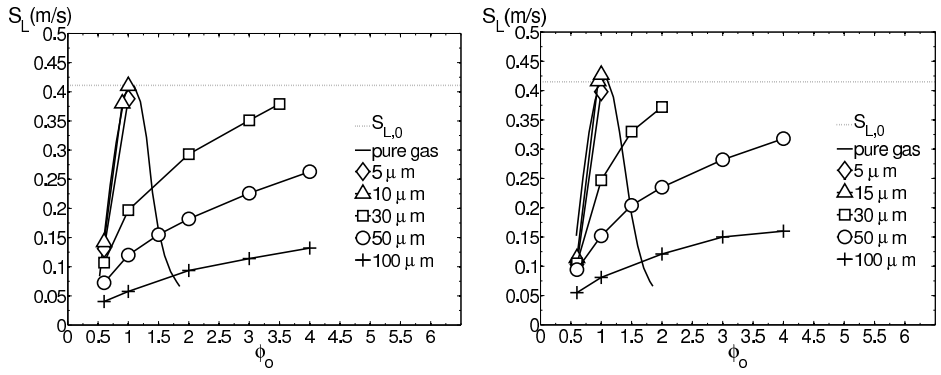


Figure 5: Calculations of laminar flame speed in n-decane sprays with detailed chemistry and assuming a uniformly-dispersed droplet mist. Left: 100 kPa, 300 K. Right: 41.65 kPa, 265 K. $S_{L,0}$ is the laminar burning velocity of the planar stoichiometric gaseous flame. From [44]. Reproduced with permission from Elsevier.

However, the flame speed in *sprays* under high-altitude conditions (low pressure, low temperature) may not be as slow as first thought. Figure 5 shows laminar flame calculations of flames in droplet mists with detailed chemistry [44]. The thermophysical properties and chemistry of n-decane has been used as surrogate for kerosene; although not all the characteristics of kerosene can be reproduced, n-decane has a high boiling point and has a similar flame speed, hence the effects of high-altitude conditions (low pressure, low temperature) are reasonably reproduced. It is evident from the calculations that the flame speeds are very similar between ambient and

relight conditions. The low temperature decreases flame speed and evaporation, but the low pressure increases flame speed and evaporation, with the net effect on flame speed being small. Note in Fig. 5 the detrimental effect of increasing droplet size and the fact that overall very rich sprays can still result in significant flame speeds.

Experiments at high-altitude conditions and in realistic geometries include those of Refs. [103, 33, 35, 34], who showed that not all sparks result in full flame ignition, that the successful ignitions are those with upstream flame capture by the recirculating flow, and that the time needed to stabilize the flame is tens of milliseconds (i.e. many combustor residence times). These findings are fully consistent with the results from the more "academic", simple-geometry, atmospheric-pressure experiments with gaseous and liquid fuels [3, 4]. Concerning the MIE, the original work of Ballal and Lefebvre, reviewed in Ref. [51], contained some low-pressure but not many low-temperature experiments. A recent experiment with kerosene at temperatures down to 250 K has shown that the MIE predicted by the theory of Ref. [51] is larger than the measured value by a large factor and that the energy needed to produce a self-sustaining (propagating flame) is larger than the MIE needed to create a kernel [104]. It seems that more work is needed both for the MIE and for a careful distinction between kernel and flame at relight conditions.

Ignition in gas turbines is usually accomplished by surface-discharge igniters that deposit large amounts of energy repeatedly over long periods of time (of the order of seconds) and create large sparks that penetrate into the flow [105, 103, 33, 35, 34]. However, flame propagation and establishment is not always achieved, despite the successful creation of an ignition kernel. This may have to do with subsequent flame propagation and spreading by the turbulent recirculating flow, further motivating studies on the fundamental problem of flame propagation and extinction in turbulent sprays that was discussed in Section 3. Also, further experiments are needed in order to assess better the effect of fuel spray placement relative to the spark.

Ignition of model gas turbine combustors has been studied with emphasis on global features of the ignition process, on the effects of the spray parameters such as the nature of the fuel and droplet size, and on the pressure and air temperature [106, 107, 108, 109, 110, 111, 112, 113]. Visualization showed that the spark creates a kernel that slowly decreases in luminosity and eventually the whole combustor would ignite giving again a bright image [109, 113]; this behaviour has been referred to as "ignition delay"

[109] (which should not be confused with the autoignition delay time of a flammable mixture) and has also been observed in laboratory-scale methane flames [3]. Consistent with our expectations from laminar spray ignition and flame propagation, gas turbine combustor ignition was easier when the kinetics were fast, the droplets small, the fuel volatile, and the air flow rate low.

Laser ignition has also been used [111, 113, 16], which is being proposed as a method that may promote ignitability due to the fact that the spark can be placed where it has a higher chance of initiating a flame, such as inside the spray (e.g. Fig. 4). Some ignition probability data with laser sparks in swirling spray flames have been reported [111, 114], which show large spatial variations in the ignition probability. The internal locations that provide the best ignitability with laser ignition in a kerosene gas turbine combustor [114] are quite similar to the ones observed in the simpler swirl flame by Marchione et al. [4].

### *4.2. Phase 4: Light-round*

After the combustor has ignited in a gas turbine engine, through interconnecting passages in "canular" designs or the inter-burner region in annular systems, the flame jumps from burner to burner across the periphery of the engine [2], which results in complete *light-round*. This process can take significant time relative to the combustor residence time. This phase of ignition has been very little studied (at least, concerning available information in the open literature) and more research is necessary. An effort to predict computationally the light-round phase has been made [115] for a helicopter engine with large-scale parallel calculations. The gas expansion following successful ignition of a single burner helps the flame spreading to the adjacent burners.

Focused experiments on this phase have provided interesting insights. First, a linear configuration with five nominally non-premixed burners (which, however, produce very quick mixing) has been studied experimentally and with LES [116]. The results show that the distance between burners (or "injectors" in gas turbine engineering terminology) has an impact on the flame pattern as the ignition process evolves from burner to burner, with a balance between the streamwise convection by the mean flow and the span-wise propagation along flammable-mixture "bridges" between burners. Volumetric expansion is also a factor that determines the flame position relative to the combustor, although this mechanism cannot explain the ignition process of

the incoming fresh gases of the adjacent, un-ignited burner; ignition necessitates diffusion. Second, an annular geometry with premixed flames [117, 118] has been studied by experiment and LES and the result shows that, again, the flame expansion process is to some extent related to volumetric expansion, and that the combustion model (and hence flame propagation model) also play a role in predicting accurately the flame behaviour. Finally, a series of non-premixed flames in an annular configuration has also been examined [119] and the overall light-round speed has been found to be very slow and depending on the emergence of connecting regions with flammable material between the burners. Similar experiments with sprays must be performed.

## 5. Calculation methods

The usual strategy in industry when dealing with turbulent reacting flows is to use Reynolds-averaged Navier-Stokes (RANS) methods to describe the mean quantities, which are usually the quantities of engineering interest. In ignition, however, which is by nature transient and that has a significant variability in its behaviour, methods including a wide range of turbulent motions, and hence physics, are needed. Large Eddy Simulations (LES) seem ideal for capturing spark ignition and recent anectodal evidence suggests that industry indeed moves in this direction.

At present, a very significant effort is underway in many laboratories to develop and validate LES for spark ignition [115, 120, 76, 100, 101, 77, 121, 116, 118]. Most of these efforts aim at academic geometries, while work to produce the whole ignition event in gas turbines has also been made [115]. LES can offer very detailed information as to why a flame, as it grows and is captured by the flow, may develop into a fully-fledged burner ignition, or why it may quench. To account for all eventualities present in the spray flame ignition process, the sub-grid combustion model must be able to capture not only flame propagation in premixed, stratified, non-premixed (e.g. edge flames) and in sprays, but also extinction of all such flames. It is not clear if turbulent combustion modelling has reached this stage yet and so there is no evidence yet that, for example, the measured $P_{ign}$ can be captured from first principles with today's combustion LES. Focused validation against measured $P_{ker}$ and $P_{ign}$, but also in terms of turbulent flame speed in sprays, is necessary before we can fully trust LES for spark ignition in spray systems.

An alternative modelling strategy is to use low-order, physics-based models. In this category, we can put modelling efforts that do not rely on full, multi-dimensional CFD simulations of the ignition process, which are obviously very expensive. Despite the expected inaccuracy, such efforts are very useful for engine developers because they can provide quick answers on the ignition behaviour of a combustor. The main approach currently for simplified modelling of ignition relies on performing a *cold flow* CFD solution, i.e. without combustion, which is relatively easier to get compared to the CFD simulation of the ignition. Then, this solution (flow pattern, spray pattern etc.) is "interrogated" in order to provide information on whether a given spark from a given location would be successful or not.

Wilson et al. [122] suggested the following procedure for investigating possible ignition in a combustor. A CFD solution of the cold flow was de-

veloped and the local Karlovitz number was estimated. A passive scalar was assumed to mix from the spark and the combination of this and the Karlovitz number gave some insights whether the spark could grow into a full flame or not. Neophytou et al. [123] extended these ideas and introduced stochasticity into both the movement of possible kernels from the spark (now assumed to follow a turbulent random walk) and the Karlovitz number, with the result that the experimentally-observed ignition probability in simple geometries was successfully predicted. The model was also used for analyzing a CFD solution of a Rolls-Royce combustor for which ignition data are available [34] and the model predicted the correct optimum placement of the spark and the time of overall burner ignition [124]. The code is named SPINTHIR (for: Stochastic Particle INTegrator for HIgh-altitude Relight) and can be adapted easily to any CFD solution. It has also been used for fully premixed single-burner and multiple-burner configurations [40, 125]. Similar efforts are also underway in many laboratories [126, 127].

## 6. Conclusions

The spark ignition of turbulent sprays shows very complex behaviour. This behaviour can be partly understood in a hierarchical manner, building up from knowledge on spark ignition of laminar and turbulent fully-premixed mixtures, to ignition of laminar strained non-premixed flames, to ignition of turbulent non-premixed flames, and then to ignition of uniformly-dispersed spray, spray mixing layer, and recirculating spray flames. Most of these canonical spray combustion problems still need extensive research from both an experimental and simulation perspective and the effects of turbulence are not fully understood. In particular, DNS with complex chemistry and a range of spray and turbulence parameters, focusing on the initial ignition phase and the subsequent turbulent flame propagation mechanism, must be performed. Experiments with simultaneous imaging of the spray parameters, equivalence ratio, and flame evolution would be fruitful for fully understanding the reasons kernels fail or succeed. Turbulent flame propagation in sprays is a key phenomenon in spray burner ignition and has been very little studied so far.

Modelling of spark ignition in spray combustors has advanced significantly the past few years, due to a combined research into the fundamentals, but also due to the increased availability of computing power that allowed Large Eddy Simulations of the whole ignition event in realistic combustors. However, the underlying physics that must be captured by the sub-grid combustion model is extensive and remains, to a large part, unvalidated. The combustion model must be able to do a good job for flame propagation and extinction in premixed, non-premixed, and spray systems, which implies multi-mode combustion with significant finite-rate kinetics. The spark itself (i.e. the plasma and its interaction with the fluid and the embryonic flame) are also receiving attention and this is a research area that must grow. Novel low-order models have been developed that can predict reasonably well the ignition probability and offer insights into the most effective spark placement in the combustor, given a CFD solution of the cold flow field. Such models are useful, but contain various approximations that need further validation.

## Acknowledgements

The work of the author in this area has been funded by the European Commissions, the Engineering and Physical Sciences Research Council, and Rolls-Royce Group. Thanks are due to Drs. A. Giusti and M. Kotzagianni

and Profs. S. Candel, N. Chakraborty, G.B. Greenberg, S. Menon, and V. Sick for the provision of data and useful comments. Some parts of this paper concerning gas turbine relight were part of VKI Lecture Notes 2010-03.

## References


[1] E. Mastorakos, Progress in Energy and Combustion Science 35 (2009) 57 – 97.

[2] A. H. Lefebvre, 2nd Edition, Taylor & Francis, 1998.

[3] S. Ahmed, R. Balachandran, T. Marchione, E. Mastorakos, Combustion and Flame 151 (2007) 366–385.

[4] T. Marchione, S. F. Ahmed, E. Mastorakos, Combustion and Flame 156 (2009) 166–180.

[5] S. Aggarwal, Progress in Energy and Combustion Science 45 (2014) 79–107.

[6] G. Borghesi, E. Mastorakos, Combustion and Flame 162 (2015) 2544–2560.

[7] E. S. Richardson, E. Mastorakos, Combustion Science and Technology 179 (2007) 21–37.

[8] J. Greenberg, L. Kagan, G. Sivashinsky, Combustion Theory and Modelling 17 (2013) 1053–1066.

[9] N. Chakraborty, E. Mastorakos, R. Cant, Combustion Science and Technology 179 (2007) 293–317.

[10] N. Chakraborty, E. Mastorakos, Flow Turbulence and Combustion 80 (2008) 155–186.

[11] N. Chakraborty, H. Hesse, E. Mastorakos, Combustion Science and Technology 182 (2010) 1747–1781.

[12] A. Wandel, N. Chakraborty, E. Mastorakos, Proceedings of the Combustion Institute 32 (2009) 2283–2290.

[13] A. Wandel, Combustion and Flame 161 (2014) 2579–2600.

[14] S. F. Ahmed, E. Mastorakos, Combustion and Flame 146 (2006) 215–231.

[15] S. F. Ahmed, R. Balachandran, E. Mastorakos, Proceedings of the Combustion Institute 31 (2007) 1507–1513.

[16] C. Letty, E. Mastorakos, A. R. Masri, M. Juddoo, W. OLoughlin, Experimental Thermal and Fluid Science 43 (2012) 47–54.

[17] B. Peterson, D. Reuss, V. Sick, Proceedings of the Combustion Institute 33 (2011) 3089–3096.

[18] B. Peterson, D. Reuss, V. Sick, Combustion and Flame 161 (2014) 240–255.

[19] D. B. Spalding, Pergamon Press, 1979.

[20] I. Glassman, 3rd Edition, Academic Press, 1996.

[21] J. Kariuki, J. Dawson, E. Mastorakos, Combustion and Flame 159 (2012) 2589–2607.

[22] J. Kariuki, A. Dowlut, R. Yuan, R. Balachandran, E. Mastorakos, Proceedings of the Combustion Institute 35 (2015) 1443–1450.

[23] D. Bradley, F. K. Lung, Combustion and Flame 69 (1987) 71–93.

[24] M. Dunn, A. Masri, R. Bilger, Combustion and Flame 151 (2007) 46–60.

[25] B. Zhou, C. Brackmann, Z. Li, M. Alden, X.-S. Bai, Proceedings of the Combustion Institute 35 (2015) 1409–1416.

[26] W. O'Loughlin, A. Masri, Combustion and Flame 158 (2011) 1577–1590.

[27] J. Driscoll, Progress in Energy and Combustion Science 34 (2008) 91–134.

[28] D. Patel, N. Chakraborty, Combustion Theory and Modelling 18 (2014) 627–651.

[29] A. Masri, Proceedings of the Combustion Institute 35 (2015) 1115–1136.

[30] A. Sanchez, J. Urzay, A. Linan, Proceedings of the Combustion Institute 35 (2015) 1549–1577.

[31] G. Gebel, T. Mosbach, W. Meier, M. Aigner, Combustion and Flame 162 (2015) 1599–1613.

[32] S. Lee, H. Do, J. Yoh, Combustion and Flame 165 (2016) 334–345.

[33] R. W. Read, J. W. Rogerson, S. Hochgreb, AIAA Journal 48 (2010) 1916–1927.

[34] T. Mosbach, R. Sadanandan, W. Meier, R. L. G. M. Eggels, In: Proc. ASME Turbo Expo 2010, Glasgow, UK, 14 - 18 June.

[35] A. Lang, R. Lecourt, F. Giuliani, ASME2010-23229.

[36] A. Neophytou, E. Mastorakos, R. Cant, Combustion and Flame 157 (2010) 1071–1086.

[37] S. Ahmed, E. Mastorakos, Combustion Science and Technology 182 (2010) 1360–1368.

[38] M. Cordier, A. Vandel, G. Cabot, B. Renou, A. Boukhalfa, Combustion Science and Technology 185 (2013) 379–407.

[39] S. Ahmed, Fuel 134 (2014) 97–106.

[40] M. Sitte, E. Bach, J. Kariuki, H.-J. Bauer, E. Mastorakos, Combustion Theory and Modelling 20 (2016) 548–565.

[41] A. Kourmatzis, P. X. Pham, A. Masri, Combustion and Flame 162 (2015) 978–996.

[42] J. Gounder, A. Kourmatzis, A. Masri, Combustion and Flame 159 (2012) 3372–3397.

[43] S. H. Starner, J. Gounder, A. Masri, Combustion and Flame 143 (2005) 420–432.

[44] A. Neophytou, E. Mastorakos, Combustion and Flame 156 (2009) 1627–1640.

[45] C. Pichard, Y. Michou, C. Cauveau, I. Gokalp, Proceedings of the Combustion Institute 29 (2002) 527–533.

[46] D. Wacks, N. Chakraborty, E. Mastorakos, Flow, Turbulence and Combustion 96 (2016) 573–607.

[47] A. Neophytou, E. Mastorakos, R. Cant, Combustion and Flame 159 (2012) 641–664.

[48] B. Lewis, G. von Elbe, Academic Press, 1987.

[49] M. Baum, T. J. Poinsot, Combustion Science and Technology 106 (1995) 19–39.

[50] C. Strozzi, P. Gillard, J.-P. Minard, Combustion Science and Technology 186 (2014) 1562–1581.

[51] D. R. Ballal, A. H. Lefebvre, Proceedings of the Combustion Institute 18 (1981) 1737–1746.

[52] P. Bowen, L. Cameron, Transactions of the Institute of Chemical Engineers 77B (1999) 22–30.

[53] B. Sforzo, J. Kim, A. Lambert, J. Jagoda, S. Menon, J. Seitzman, Combustion and Flame 162 (2015) 161–190.

[54] R. Dahms, T. Fansler, M. Drake, T.-W. Kuo, A. Lippert, N. Peters, Proceedings of the Combustion Institute 32 (2009) 2743–2750.

[55] I. Mulla, A. Chakravarthy, N. Swaminathan, R. Balachandran, Combustion and Flame 164 (2016) 303–318.

[56] K. Miki, J. Schulz, S. Menon, Proceedings of the Combustion Institute 32 (2009) 2413–2420.

[57] M. Castela, B. Fiorina, A. Coussement, O. Gicquel, N. Darabiha, C. Laux, Combustion and Flame 166 (2016) 133–147.

[58] G. Gebel, T. Mosbach, W. Meier, M. Aigner, S. Le Brun, Journal of Engineering for Gas Turbines and Power 135 (2013) 021505–1.

[59] N. Chakraborty, E. Mastorakos, Physics of Fluids 18 (2006) 105103.

[60] N. Charkraborty, E. Mastorakos, R. S. Cant, Combustion Science and Technology 179 (2007) 293–317.

[61] A. D. Birch, D. R. Brown, M. G. Dodson, Proceedings of the Combustion Institute 18 (1981) 1755–1780.

[62] C. E. Polymeropoulos, S. Das, Combustion and Flame 25 (1975) 247–257.

[63] A. K. Singh, C. E. Polymeropoulos, Proceedings of the Combustion Institute 21 (1986) 513–519.

[64] A. M. Danis, I. Namer, N. P. Cernansky, Combustion and Flame 74 (1988) 285–294.

[65] D. L. Dietrich, N. P. Cernansky, M. B. Somashekara, I. Namer, Proceedings of the Combustion Institute 23 (1990) 1383–1389.

[66] S. D. Wehe, N. Ashgriz, Combustion Science and Technology 86 (1992) 45–65.

[67] H. T. Sommer, Proceedings of the Combustion Institute 21 (1986) 641–646.

[68] S. K. Aggarwal, W. A. Sirignano, Proceedings of the Combustion Institute 20 (1984) 1773–1780.

[69] D. R. Ballal, A. H. Lefebvre, Combustion and Flame 31 (1978) 115–126.

[70] S. K. Aggarwal, Progress in Energy and Combustion Science 24 (1998) 565–600.

[71] D. R. Ballal, A. H. Lefebvre, Proceedings of the Combustion Institute 15 (1976) 1473–1481.

[72] D. R. Ballal, A. H. Lefebvre, Proc. Roy. Soc. Lond. A 357 (1977) 163–181.

[73] D. R. Ballal, A. H. Lefebvre, Combustion and Flame 35 (1979) 155–168.

[74] G. Kats, J. Greenberg, AIAA SciTech 2016 Paper 2016-1209.

[75] J. L. McCraw, N. J. Moore, K. M. Lyons, Flow Turbulence Combust. 79 (2006) 83–97.

[76] G. Lacaze, E. Richardson, T. Poinsot, Combustion and Flame 156 (2009) 1993–2009.

[77] W. P. Jones, V. N. Prasad, Proceedings of the Combustion Institute 33 (2011) 1355–1363.

[78] X. Qin, C. W. Choi, A. Mukhopadhyay, I. K. Puri, S. K. Aggarwal, V. R. Katta, Combustion Theory and Modelling 8 (2004) 293–314.

[79] Y. S. Ko, S. H. Chung, Combustion and Flame 118 (1999) 151–163.

[80] J. Buckmaster, Progress in Energy and Combustion Science 28 (2002) 435–475.

[81] T. Echekki, J. H. Chen, Combustion and Flame 114 (1998) 231–245.

[82] C. Heeger, B. Boehm, S. F. Ahmed, R. Gordon, I. Boxx, W. Meier, A. Dreizler, E. Mastorakos, Proceedings of the Combustion Institute 32 (2009) 2957–2964.

[83] H. Hesse, N. Chakraborty, E. Mastorakos, Proceedings of the Combustion Institute 32 (2009) 1399–1407.

[84] J. Greenberg, Combustion and Flame 148 (2007) 187–197.

[85] D. R. Ballal, A. H. Lefebvre, Proceedings of the Combustion Institute 18 (1981) 321–328.

[86] H. Nomura, I. Kawasumi, Y. Ujiie, J. Sato, Proceedings of the Combustion Institute 31 (2007) 2133–2140.

[87] F. Atzler, F. Demoulin, M. Lawes, Y. Lee, N. Marquez, Combustion Science and Technology 178 (2006) 2177–2198.

[88] J. B. Greenberg, I. Silverman, Y. Tambour, Combustion and Flame 113 (1998) 271–273.

[89] A. Dvorjetski, J. Greenberg, Proceedings of the Combustion Institute 28 (2000) 1047–1054.

[90] A. Dvorjetski, J. Greenberg, Proceedings of the Combustion Institute 32 (2009) 2205–2214.

[91] J. Greenberg, A. Dvorjetski, Combustion Theory and Modelling 7 (2003) 145–162.

[92] C. Nicoli, P. Haldenwang, B. Denet, Flow, Turbulence and Combustion To appear.

[93] T. Niioka, Combustion Science and Technology 177 (2005) 1167–1182.

[94] W. Han, Z. Chen, Combustion and Flame 162 (2015) 2128–2139.

[95] N. K. Kopyt, A. Struehaev, Y. I. Krasnoshchekov, N. Rogov, K. N. Shamshev, Combustion, Explosion and Shock Waves 25 (1989) 279–285.

[96] G. D. Myers, A. H. Lefebvre, Combustion and Flame 66 (1986) 193–210.

[97] G. A. Richards, A. H. Lefebvre, Combustion and Flame 78 (1989) 229–307.

[98] M. Lawes, Y. Lee, A. Mokhtar, R. Woolley, Combustion Science and Technology 180 (2008) 296–313.

[99] S. Marley, K. Lyons, K. Watson, Flow, Turbulence and Combustion 72 (2004) 29–47.

[100] A. Triantafyllidis, E. Mastorakos, R. L. G. M. Eggels, Combustion and Flame 156 (2009) 2328–2345.

[101] V. Subramanian, P. Domingo, L. Vervisch, Combustion and Flame 157 (2010) 579–601.

[102] M. Zhu, B. Rogg, Meccanica 31 (1996) 177–193.

[103] R. W. Read, J. W. Rogerson, S. Hochgreb, Paper AIAA-2008-0957.

[104] M. Majcherczyk, N. Zarzalis, F. Turrini ASME Paper GT2014-25332.

[105] N. Ouarti, Ph.D. thesis, Ecole Nationale Superieur de l'Aeronautique et de l'Espace, ONERA (2004).

[106] A. M. Mellor, Progress in Energy and Combustion Science 6 (1980) 347–358.

[107] J. E. Peters, A. M. Mellor, AIAA Journal 6 (1982) 272–274.

[108] A. H. Lefebvre, Journal of Engineering for Gas Turbines and Power 107 (1985) 24–37.

[109] D. W. Naegeli, L. G. Dodge, Combustion Science and Technology 80 (1991) 165–184.

[110] N. Y. Sharma, A. Datta, S. K. Som, Applied Thermal Engineerins 21 (2001) 1755–1768.

[111] H. El-Rabii, K. Zähringer, J. Rolon, F. Lacas, Combustion Science and Technology 176 (2004) 1391–1417.

[112] Y. Levy, V. Sherbaum, V. Nadvany, Y. Nehkamkin, Journal of Propulsion and Power 22 (2006) 828–834.

[113] S. Barbosa, P. Scouflaire, S. Ducruix, G. Gaborel, in: Third European Combustion Metting, Combustion Institute, Crete, Greece, 2007.

[114] K. Moesl, K. Vollmer, T. Sattelmayer, J. Eckstein, H. Kopecek, Journal of Engineering for Gas Turbines and Power 131 (2009) 021501–1.

[115] M. Boileau, G. Staffelbach, B. Cuenot, T. Poinsot, C. Berat, Combustion and Flame 154 (2008) 2–22.

[116] D. Barre, L. Esclapez, M. Cordier, E. Riber, B. Cuenot, G. Staffelbach, B. Renou, A. Vandel, L. Gicquel, G. Cabot, Combustion and Flame 161 (2014) 2387–2405.

[117] J.-F. Bourgouin, D. Durox, T. Schuller, J. Beaunier, S. Candel, Combustion and Flame 160 (2013) 1398–1413.

[118] M. Philip, M. Boileau, R. Vicquelin, E. Riber, T. Schmitt, B. Cuenot, D. Durox, S. Candel, Proceedings of the Combustion Institute 35 (2015) 3159–3166.

[119] E. Machover, E. Mastorakos, Experimental Thermal and Fluid Science 73 (2016) 64–70.

[120] G. Lacaze, B. Cuenot, T. Poinsot, M. Oschwald, Combustion and Flame 156 (2009) 1166–1180.

[121] W. P. Jones, A. Tyliszczak, Flow Turbulence and Combustion 85 (2010) 711–734.

[122] C. W. Wilson, C. G. W. Sheppard, H. C. Low, In: Applied Vehicle Technology Panel Symposium, Lisbon, Portugal.

[123] A. Neophytou, E. Richardson, E. Mastorakos, Combustion and Flame 159 (2012) 1503 – 1522.

[124] A. Neophytou, E. Mastorakos, E. Richardson, S. Stow, M. Zedda, In: Mediterranean Combustion Symposium, Chia Laguna, Sardinia, 11 - 15 September.

[125] E. R. Machover, Ph.D. thesis, University of Cambridge (2016).

[126] L. Esclapez, E. Riber, B. Cuenot, Proceedings of the Combustion Institute 35 (2015) 3133–3141.

[127] A. Eyssartier, B. Cuenot, L. Gicquel, T. Poinsot, Combustion and Flame 160 (2013) 1191–1207.